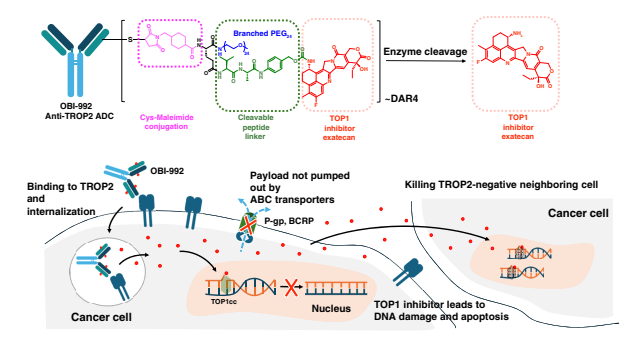
OBI-992, a Novel TROP2-Targeted Antibody-Drug Conjugate, Demonstrates Antitumor Activity in Multiple Cancer Models



Wan-Fen Li, Ming-Feng Chiang, Hao-Cheng Weng, Jhih-Jie Yang, Hsin-Shan Wu, Szu-Yu Wu, Yu-Jung Chen, Chi-Huan Lu, Jyy-Shiuan Tu, Ren-Yu Hsu, Chi-Sheng Shia, Teng-Yi Huang, and Ming-Tain Lai

ABSTRACT

Trophoblast cell surface antigen 2 (TROP2) is highly expressed in multiple cancers relative to normal tissues, supporting its role as a target for cancer therapy. OBI-992 is an antibody-drug conjugate (ADC) derived from a novel TROP2targeted antibody linked to the topoisomerase 1 (TOP1) inhibitor exatecan via an enzyme-cleavable hydrophilic linker, with a drug-antibody ratio of 4. This study evaluated and compared the antitumor activity of OBI-992 with that of benchmark TROP2targeted ADCs datopotamab deruxtecan (Dato-DXd) and sacituzumab govitecan (SG) in cell line-derived xenograft (CDX) and patient-derived xenograft (PDX) models. OBI-992 treatment exhibited statistically significant antitumor activity versus controls at doses of 3 and 10 mg/kg in various CDX and PDX models, demonstrating comparable or better antitumor activity with benchmark ADCs. In a large-tumor model, longer survival times were observed in OBI-992-treated mice compared with Dato-DXd-treated mice. OBI-992 treatment induced marked bystander killing of TROP2-negative cells in the presence of nearby TROP2-positive cells in both in vitro and in vivo studies. In lung adenocarcinoma CDX models with overexpression of either P-glycoprotein (P-gp) or breast cancer resistance protein (BCRP) to mimic ATP-binding cassette transporter-mediated multidrug resistance, OBI-992 treatment maintained antitumor activity when Dato-DXd treatment became less effective. The combination of OBI-992 at suboptimal doses with either poly (ADP-ribose) polymerase (PARP) inhibitors or an immune check point inhibitor produced synergistic antitumor effects in mouse models. Taken together, these translational results support further development of OBI-992 as a cancer therapy.



Introduction

Antibody-drug conjugates (ADC) consist of a tumor-specific monoclonal antibody connected via a chemical linker to a cytotoxic payload, allowing targeted delivery of potent cytotoxic drugs (1, 2). This approach improves the therapeutic index of anticancer therapies and has been under intense research in recent years, with dozens of combinations of antibodies targeting various antigens and anticancer payloads leveraged in preclinical and clinical studies (1, 2). One target for anticancer drug delivery is trophoblast cell surface antigen 2 (TROP2), a transmembrane glycoprotein that is overexpressed in various tumor types relative to normal tissues (3, 4).

OBI Pharma, Inc., Taipei, Taiwan.

Corresponding Author: Ming-Tain Lai, OBI Pharma, Inc., 6F, No. 508, Section 7, Zhongxiao East Road, Nangang District, Taipei City 115011, Taiwan; E-mail: mingtainlai@obipharma.com

Mol Cancer Ther 2024;XX:XX-XX

doi: 10.1158/1535-7163.MCT-24-0588

This open access article is distributed under the Creative Commons Attribution-NonCommercial-NoDerivatives 4.0 International (CC BY-NC-ND 4.0) license.

©2024 The Authors; Published by the American Association for Cancer Research

TROP2 is involved in stem cell biology, and its upregulation in tumor cells promotes the activation of downstream signaling networks that enhance cell survival, proliferation, migration, and invasion (4–8). Overexpression of TROP2 correlates with poor prognosis of several cancers, including oral, pancreatic, gastric, gallbladder, and breast (9–13).

Topoisomerase 1 (TOP1) inhibitors have long been investigated as cytotoxic agents. Exatecan is a potent TOP1 inhibitor that does not require metabolic activation and is a poor substrate for multidrug resistance ATP-binding cassette (ABC) transporters (14), such as breast cancer resistance protein (BCRP) and P-glycoprotein (P-gp). Exatecan has been studied as a single agent in several clinical trials for its safety, pharmacokinetics, and efficacy in cancer treatment (15–17) and has been identified as a promising ADC payload (18).

The ADC pairing of a TROP2-targeted antibody with a TOP1 inhibitor has demonstrated success as a cancer therapy, with sacituzumab govitecan (SG) as the first approved TROP2-targeted ADC with the TOP1 inhibitor SN-38 as the payload (19). However, SG has a short half-life due to its unstable linker and requires frequent dosing on days 1 and 8 per 21-day treatment cycle (20). Furthermore, SN-38 undergoes glucuronide-mediated metabolism that can cause severe diarrhea or an increased risk for neutropenia



(21). Datopotamab deruxtecan (Dato-DXd) is an investigational TROP2-targeted ADC with improved pharmacokinetics and less frequent dosing (once every 21-day cycle) than SG. Trastuzumab deruxtecan and Dato-DXd use the same DXd-ADC linker/payload platform, and both ADCs have been linked to interstitial lung disease (22, 23). Therefore, a stable linker may improve the ADC's pharmacokinetics and lowers off-target toxicities, but it may also increase on-target toxicities if the target antigen is also expressed in normal tissues.

OBI-992 is an ADC derived from a novel anti-TROP2 antibody, which binds to a region distinct from that of sacituzumab and datopotamab, linked with exatecan via a hydrophilic enzymecleavable linker at a DAR of 4. The hydrophilic linker includes a protease-sensitive peptide (MCCa-PEG24-VA-PAB-exatecan) that is covalently bonded to cysteine residues of the antibody (T.L. Chang and colleagues; submitted for publication). Ex vivo serum stability and in vitro cytotoxicity studies demonstrated that OBI-992 has a more stable linker and lower toxicity than Dato-DXd, warranting further investigation of OBI-992 activity in vivo (24). In this study, we evaluated the antitumor activity of OBI-992 in cancer cell line-derived xenograft (CDX) and patient-derived xenograft (PDX) models of various types of solid tumors in comparison with SG and Dato-DXd. Additionally, we assessed the bystander killing effect of OBI-992 and OBI-992 antitumor activity in a model with overexpression of ABC transporters, a common mechanism of ADC resistance. Finally, we evaluated the synergistic antitumor effects of combined OBI-992 with established cancer therapies.

Materials and Methods

Refer to Supplementary Methods for details on the characterization of OBI-992, liquid chromatography/tandem mass spectrometry (LC/MS-MS), and immunogenic cell death (ICD) assays.

Reagents

SG was purchased from Gilead Sciences. SN-38, MMAE, DXd, and exatecan were purchased from Acros Organics, BroadPharm, MedChemExpress, and Seedchem, respectively. P-gp inhibitor verapamil hydrochloride and BCRP inhibitor Ko143 were purchased from Acros Organics and TargetMol, respectively. Olaparib and talazoparib were purchased from Combi-Blocks and Ambeed. Digoxin and estrone 3-sulfate potassium salt were purchased from Sigma-Aldrich.

Preparation of OBI-992 and Dato-DXd

The OBI-992 and a control ADC (human IgG1-exatecan conjugate) were produced in house as described previously (T.L. Chang and colleagues; submitted for publication). Briefly, the anti-TROP2 antibody R4702 and human IgG1 isotype control (BE0297, BioXcell) in conjugation buffer (50 mmol/L histidine, 20 mmol/L ethylenediaminetetraacetic acid, pH 7.0) were treated with tris(2-carboxyethyl) phosphine hydrochloride for 2 to 6 hours to reduce the disulfide bond of the antibodies. The reduced antibodies were incubated with molecules containing maleimide-PEG24-VA-PAB-exatecan for 1 hour to complete the conjugation. Next, the conjugation buffer was replaced by storage buffer [20 mmol/L sodium acetate, pH 5.0 with 0.1% (w/w) polysorbate 80] via ultrafiltration/diafiltration to create final ADC OBI-992 and control ADC solutions. Drug load distribution (DLD) of the ADC was determined by hydrophobic interaction chromatography, and drug-antibody ratio (DAR) was

measured and calculated by reduced reversed-phased HPLC-UV (RPLC-UV). The calculation of average DAR is described in Supplementary Methods. The average DAR value was 3.9 for OBI-992 and 5.1 for the control ADC. The amino acid sequences of the anti-TROP2 antibody, R4702, are provided in Supplementary Fig. S1A and S1B. The full chemical structure of OBI-992 is illustrated in Supplementary Fig. S1C.

Dato-DXd was produced as described in the Patent US2021/ 0386865 A1 (25). The DLD of OBI-produced Dato-DXd was assessed using hydrophobic interaction chromatography and then compared with the DLD outlined in the patent (Supplementary Fig. S2). The average DAR of OBI-produced Dato-DXd was determined by RPLC-UV as 4.1.

Cell lines and culture

Cancer cell lines NCI-N87 (CRL-5822), BxPC-3 (CRL-1687), HCC827 (CRL-2868), NCI-H1975 (CRL-5908), and MDA-MB-231 (HTB-26) were purchased from ATCC. Capan-1 (HTB-79) was purchased from AddexBio. ES-2/GFP (SC066-G) was purchased from GenTarget. MC38 (ENH204) was purchased from Kerafast. Caco-2 (60182, C2BBe1) was obtained from BCRC. HCC827/ABCB1 (HC-0220) and HCC827/ABCG2 (HC-0210) were purchased from Creative Cell. The detailed information of each cell line (RRID, purchase date, passage number, and biological sex) is described in Supplementary Table S1. NCI-H1975, NCI-N87, BxPC-3, HCC827, and MC38 cells were cultured in RPMI-1640 supplemented with 10% FBS and 1% penicillin/ streptomycin. MDA-MB-231 and Caco-2 cells were cultured in DMEM supplemented with 10% FBS and 1% penicillin/ streptomycin. Capan-1 cells were cultured in IMDM supplemented with 20% FBS and 1% penicillin/streptomycin. ES-2/GFP cells were cultured in McCoy's 5A medium supplemented with 10% FBS, 0.1% sodium pyruvate, and 1% penicillin/streptomycin. Cells were revived from working cell banks in which cells in cryostock were approximately passages 4 to 20, depending on cell lines. Mycoplasma tests were performed after revival of the cells from cryostock using the Universal Mycoplasma Detection Kit (ATCC) to ensure all cell lines used were free of mycoplasma. After resuscitation, cells were passaged three to five times before use. For in vitro studies, cells were cultured for 1 week before treatment. For in vivo xenograft studies, cells were cultured for 2 to 4 weeks before implantation. Caco-2 cells were passaged 10 times before being used in permeability test.

Cell-based cytotoxicity assay

Cancer cells were seeded in a 96-well plate at a density of 3,000 cells/well. After overnight incubation, cells were treated with serially diluted reagents. After treatment for 6 days, cell viability was analyzed using CellTiter-Glo (Promega) according to the manufacturer's instructions. Briefly, the CellTiter-Glo reagent was added to the culture medium at a 1:1 ratio and mixed on an orbital shaker for 2 minutes. The plate was incubated at room temperature for an additional 10 minutes before luminescence signals were measured using SpectraMax L (Molecular Devices). IC50 values were calculated using Prism (GraphPad).

The synergistic biologic activity was analyzed by the coefficient of drug interaction (CDI), which was calculated as CDI = $AB/(A \times B)$. According to the cell viability of each group, AB is the ratio of the combination groups to control group, and A or B is the ratio of the single agent group to control group. Thus, a CDI value of <1, =1,

or >1 indicates that the drugs are synergistic, additive, or antagonistic, respectively (26).

Flow cytometry and quantitative flow cytometry

The TROP2 cell surface expression levels in cancer cell lines were determined by flow cytometry using a BD Canto II flow cytometer as previously described (27). Briefly, cells were stained with the native antibody R4702 for 30 minutes on ice and then incubated with antihuman IgG Fc-FITC (F9512, Sigma-Aldrich) for 30 minutes on ice. The signal intensities of cells were evaluated by flow cytometry. Positive cells were gated based on the cells stained with antihuman IgG Fc-FITC. For quantitative flow cytometry, cells were stained with AF488-conjugated mouse antihuman TROP2 antibody (clone 77220, R&D Systems) or an isotype control antibody. The number of binding sites of the antihuman TROP2 antibody on cells was calculated using Quantum Simply Cellular anti-Mouse IgG Kit (Bangs Laboratories, Inc.) according to the manufacturer's instructions. In brief, the Quantum Simply Cellular calibration microspheres were coated with increasing amounts of capture antibody, which was the same antibody used to label cells. The fluorescence signals of the labeled calibration microspheres and cells were recorded and analyzed using the QuickCal analysis template (Bangs Laboratories, Inc.) to determine the antibody binding capacity value of each cell.

IHC staining and interpretation

Human normal tissue microarrays, FDA999w2, were obtained from US Biomax. Tissue microarrays included 32 organ types, with samples from three different individuals per organ type. Up to 448 formalin-fixed, paraffin-embedded human late-stage tumor tissue samples, representing 19 cancer types [bladder cancer, cervical adenocarcinoma, cervical squamous cell carcinoma (SCC), colorectal cancer, endometrial cancer, esophageal cancer, gallbladder cancer, gastric cancer, head and neck cancer, hormone receptorpositive (HR+) breast cancer, human epidermal growth factor receptor 2-positive (HER2+) breast cancer, non-small cell lung cancer (NSCLC) adenocarcinoma, NSCLC SCC, ovarian adenocarcinoma, pancreatic cancer, prostate cancer, renal cell carcinoma (RCC), small cell lung cancer (SCLC), and triple-negative breast cancer (TNBC)], were purchased from AMS Biotechnology. IHC staining of TROP2 was performed on Autostainer Dako Link48 and PT Link module (Dako), using rabbit antihuman TROP2 monoclonal antibody (SP294, Abcam) according to an in-house protocol. Briefly, the formalin-fixed, paraffin-embedded tissue sections were deparaffinized and pretreated with EnVision FLEX Target Retrieval Solution High pH (K8004, Dako) at 97°C for 30 minutes. Slides were then transferred to an Autostainer Dako Link to block endogenous peroxidase for 5 minutes followed by incubation with an anti-TROP2 antibody or an isotype control antibody rabbit IgG (EPR25A, Abcam) for 1 hour. Slides were developed with the En-Vision FLEX High pH kit (K8002, Dako). Lastly, the sections were counterstained with EnVision FLEX Hematoxylin (K8008, Dako) for 5 minutes and then mounted.

The IHC staining results of TROP2 expression were evaluated by a certified pathologist. The H-score system (range from 0 to 300; ref. 28) was used to evaluate the cytosolic/membranous expression of TROP2 and was calculated using the following formula: (percentage of cells with weak staining intensity \times 1) + (percentage of cells with moderate staining intensity \times 2) + (percentage of cells with strong staining intensity \times 3). Representative IHC images of TROP2 low (1+), moderate (2+), and high (3+) expression are shown in

Supplementary Fig. S3. The prevalence of TROP2 expression was calculated for each cancer type as the number of samples with an H-score ≥ 100 out of the total number of samples evaluated for that particular cancer type. For the comparison of TROP2 membranous expression in normal and tumor tissues, the percentage of viable cells showing membranous staining at any intensity was assessed.

Mouse models

The mouse studies described here were conducted at several institutions; protocols were approved by the Institutional Animal Care and Use Committee (IACUC) at the corresponding facilities. All the mouse studies using CDX models were approved by the IACUC at National Laboratory Animal Center in Taipei, Taiwan. The studies using the PDX models BR9464, GA0091, and GA6866 were approved by the IACUC at Crown Bioscience, Inc. The studies using the PDX models LU-01-1370, PC-07-0003, ES-06-0010, OV-10-0068, LU-01-1004, and LU-01-0236 were approved by the IACUC at WuXi AppTec Co., Inc. For all the mouse tumor models described, 6- to 8-week-old female mice weighing 18 to 22 g were used. In all studies, mice were divided into treatment groups based on tumor volume to achieve an equal distribution between the different dosing groups. Given the variation in tumor growth, all groups consisted of 3 to 10 mice to allow statistical comparisons between groups.

CDX models

NCI-N87, BxPC-3, MDA-MB-231, NCI-H1975, HCC827, HCC827/ABCB1(P-gp), HCC827/ABCG2 (BCRP), and Capan-1 xenograft tumor models were established to evaluate the antitumor activity of OBI-992. Tumor cells (2.5–20 × 10⁶ depending per cell line) suspended in Matrigel/saline (1:1) were subcutaneously injected into female CAnN.Cg-Foxn1^{nu}/CrlBltw (BALB/c nude) or NOD.Cg-Prkdc^{scid}Il2rg^{tm1Vst}/Vst mice (BioLasco Taiwan). Tumorbearing mice were divided into treatment groups when the tumor volume reached 150 to 250 mm³ for standard xenograft models or 450 to 550 mm³ for the BxPC-3 large-tumor model. The first treatment day was denoted as day 1. Tumor volume and mouse body weight were monitored twice weekly until the end of the study or at the humane endpoint. The tumor volume was calculated using ellipsoid equation [(major axis × minor axis × minor axis) × (π/6)].

OBI-992, Dato-DXd, and SG were administered via intravenous injection, and olaparib and talazoparib were administered by oral gavage. PBS served as the vehicle control and was administered intravenously. Antitumor activity was determined by the tumor growth inhibition (TGI) metric, which was calculated using the following formula: TGI (%) = $[1 - (\text{Ti} - \text{T1})/(\text{Ci} - \text{C1})] \times 100\%$. Ti and Ci indicate mean tumor volume in the treatment and control group, respectively, at the end of the study. T1 and C1 indicate the mean tumor volume in the treatment and control groups, respectively, on day 1.

PDX models

PDX models with TROP2 gene expression greater than 5 log₂ fragments per kilobase of transcript per million mapped reads were selected for investigation. RNA-seq data were sourced from the Crown Bioscience or WuXi Biologics databases. Breast (BR9464), pancreatic (PC-07-0003), ovarian (OV-10-0068), esophageal (ES-06-0010), gastric (GA6866 and GA0091), and non-small cell lung (LU-01-0236, LU-01-1004, and LU-01-1370) PDX cancer models were used for studying OBI-992 antitumor activity. Tumor tissues derived from patients were maintained in the host mice. Tumor

fragments (2–3 mm in diameter or 20–30 mm³) harvested from the host mice were subcutaneously implanted into BALB/c nude or NOD.CB17-Prkdc/J (NOD/SCID) mice. Tumor-bearing mice were divided into treatment groups when the tumor volume reached 150 to 200 mm³. Treatments were administered as described in the previous section. Mice were monitored, and tumor volume and TGI were calculated as described in the previous section.

Syngeneic mouse tumor model

MC38 mouse colon cancer cells were transduced with lentiviral vectors (RNAi core facility, Academia Sinica) containing human TROP2 cDNA to create MC38 cells with ectopic human TROP2 expression (MC38/hTROP cells). After transduction, pooled stable cell lines were selected using 2 μ g/mL of puromycin. Human TROP2 expression in stable cells was confirmed using flow cytometry.

An MC38/hTROP2 syngeneic tumor model was used to evaluate the antitumor activity of OBI-992 in combination with an antimouse PD-1 antibody (clone: RMP1-14, Leinco). MC38/hTROP2 cells (1×10^6 cells/mouse) suspended in Matrigel/saline (1:1) were subcutaneously injected into female C57BL/6NCrl mice, and tumor-bearing mice were divided into treatment groups when the average tumor volume reached 200 to 300 mm³. Mice were treated with a single 3 mg/kg dose of OBI-992 and/or 5 mg/kg anti-PD-1 twice weekly for three doses via intravenous injection. Tumor growth was monitored twice per week, and TGI was calculated as described previously.

Bystander effect assay

TROP2-positive BxPC-3 cells and TROP2-negative ES-2/GFP cells were used to evaluate OB-992 bystander killing effects. ES-2/ GFP cells were cultured alone or co-cultured with BxPC-3 cells at different ratios (0:1, 0.25:1, 0.5:1, 1:1, 2:1, 4:1 BxPC-3:ES-2/GFP) overnight. Serially diluted OBI-992 or control ADC (5, 2, 1, 0.5, 0 nmol/L) was added to cultures and incubated for 6 days. ES-2/ GFP cell viability was evaluated by SpectraMax M2 (Molecular Devices). The viability of the treated groups was compared with that of the corresponding untreated control (0 nmol/L). To evaluate the in vivo bystander effects, 5×10^5 ES-2/GFP cells alone or mixed with 1×10^7 BxPC-3 cells were subcutaneously injected into female BALB/c nude mice. Tumor-bearing mice were divided into treatment groups when the tumor volume reached 150 to 200 mm³. Mice were administered 3 mg/kg OBI-992 or control ADC intravenously. The mice were monitored, and tumor volume and TGI were calculated as described in the previous section. The fluorescence intensity of ES-2/GFP tumors was measured by IVIS Spectrum In Vivo Imaging System.

RNA isolation and qRT-qPCR for the assessment of ABCB1 and ABCG2 expression

Cells were lysed, and total RNA was isolated using the RNeasy Mini Kit (74104 QIAGEN) according to the manufacturer's instructions. cDNA was prepared by reverse transcription of isolated total RNA using the ReverTra Ace PCR RT Master Mix with gDNA Remover (A1172K, TOYOBO). The cDNA was subjected to qRT-PCR with KAPA SYBR FAST qPCR Kit Master Mix (2×) ROX Low (Kapa Biosystems). The relative expression of ABCB1 and ABCG2 mRNA was calculated by Ct ($\Delta\Delta$ Ct) method, and the expression in HCC827 served as a standard control. The primer sets include P-gp (ABCB1): forward-5'-GCTCCTGACTATGC-CAAAGCC-3', reverse-5'-CTTCACCTCCAGGCTCAGTCCC-3',

and BCRP (*ABCG2*): forward-5'-TGGCTTAGACTCAAGCA-CAGC-3', reverse-5'-TCGTCCCTGCTTAGACATCC-3'.

Permeability assay

All permeability assays were conducted using Caco-2 cells seeded onto 12-well Transwell inserts with a 0.4-µm pore size polycarbonate membrane at a density of 100,000 cells per insert. The cells were cultured for approximately 25 days until they formed a confluent monolayer with tight junctions. Prior to the assay, the cells were washed using prewarmed PBS and preincubated at 37°C for 15 minutes using the incubation medium of Hank's balanced salt solution with 10 mmol/L N-2-hydroxyethylpiperazine-N-2-ethane sulfonic acid. After removing the preincubated medium, for apical (AP) to basolateral (BL) permeability assays, the incubation medium containing 10 µmol/L TOP1 inhibitors (exatecan, SN-38, or DXd), digoxin, or estrone 3-sulfate with or without P-gp or BCRP inhibitors was added to the AP side, and incubation medium alone was added to the BL side, followed by incubation at 37°C for 2 hours. Conversely, for BL to AP permeability assays, the TOP1 inhibitors with or without P-gp or BCRP inhibitors were added to the BL side, and incubation medium alone was added to the AP side, followed by incubation at 37°C for 2 hours. The solutions from the AP and BL sides were collected at 0 and 2 hours for measurement of TOP1 inhibitors using LC/MS-MS. The methods and conditions of LC/MS-MS are described in Supplementary Methods.

Statistical analysis

Statistical analysis was performed using GraphPad Prism 6.01. Two-tailed unpaired t test was used to compare the vehicle group and the treatment group, as well as the OBI-992 group and benchmark group. The comparison was performed using the tumor volume of the last time point at the end of study. Statistical analyses of survival curves were performed by log-rank (Mantel-Cox) test.

Data availability

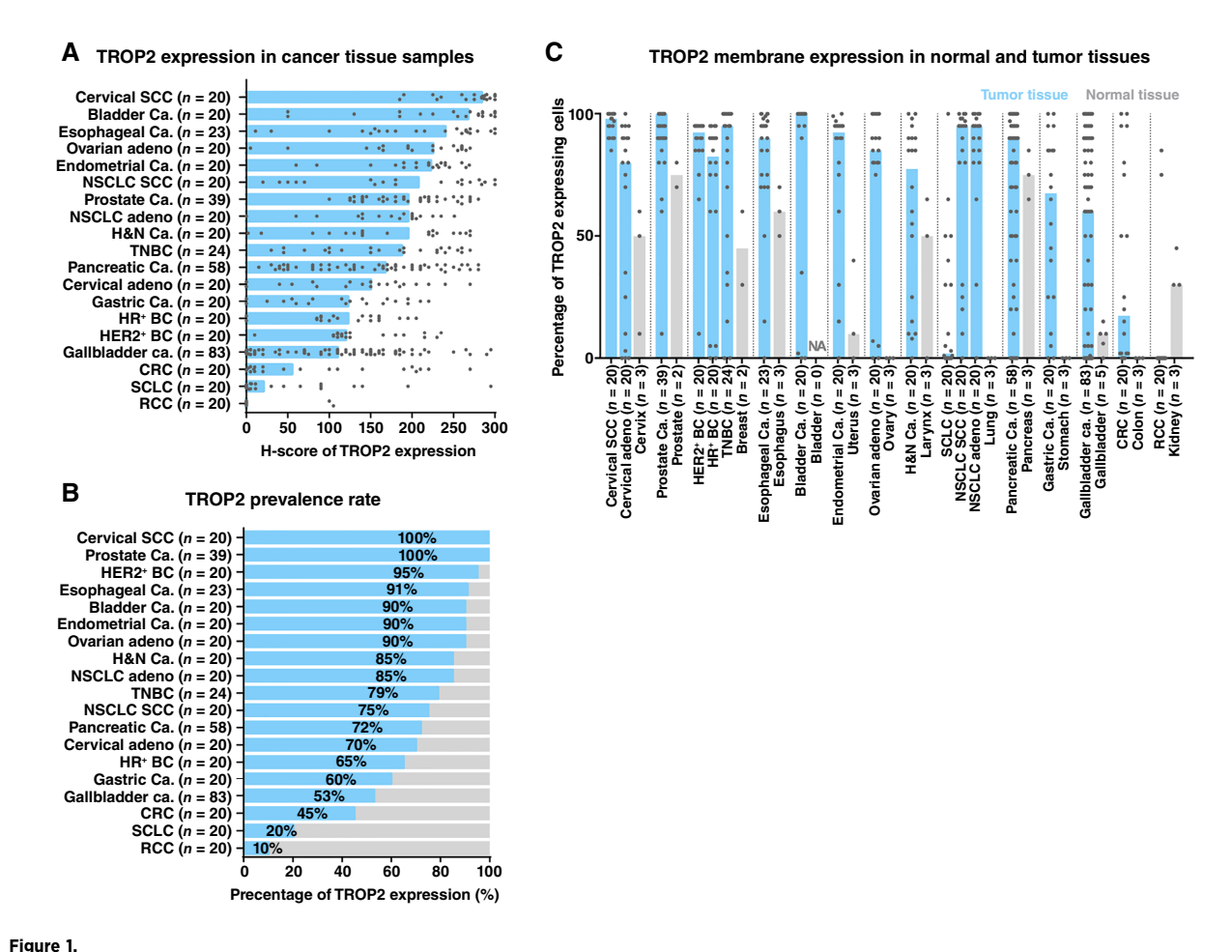
The data generated in this study are available upon request from the corresponding author.

Results

TROP2 is expressed in various cancer types

To investigate the potential therapeutic utility of OBI-992, TROP2 expression in human tissue samples from 19 types of cancer was evaluated by IHC (Fig. 1A). TROP2 prevalence was >80% in nearly half of the cancer types tested (Fig. 1B). Next, we assessed TROP2 expression at the cellular membrane in cancer tissues and corresponding normal tissues using IHC. Most of the cancer tissues tested had a higher percentage of cells with membrane TROP2 expression than the corresponding normal tissue (Fig. 1C). RCC was the only cancer type with lower TROP2 membrane expression than normal tissue.

TROP2 expression was also evaluated quantitatively in cancer cell lines by flow cytometry–based assays (Supplementary Table S2). Many cancer cell lines expressed TROP2, including pancreatic cancer (BxPC-3 and Capan-1), lung cancer (HCC827 and NCI-H1975), gastric cancer (NCI-N87), and breast cancer (MDA-MB-231). The high levels of TROP2 expression in various cancer tissues and cell lines support the preclinical testing of OBI-992.



TROP2 expression in various cancer tissues. **A,** The expression levels of TROP2 in tissue samples from 19 cancer types were analyzed by IHC. Dots indicate TROP2 *H*-score for each sample, and solid bars indicate the median *H*-score of each cancer type. **B,** TROP2 prevalence rates (*x*-axis) were calculated as the percentage of samples with TROP2 *H*-score ≥100. The ranking order of cancer types was based on the TROP2 prevalence rate. **C,** Plot of percentage of cells from tumor (blue) and corresponding normal tissues (gray) with TROP2 membrane expression determined by IHC. Each dot represents an individual sample. Solid bars indicate the median percent of TROP2-expressing cells for each tissue type. The numbers of specimens used for each cancer type are indicated in the plots. Representative IHC images of TROP2 high (3+), moderate (2+), and low (1+) expression are shown in Supplementary Fig. S3. Adeno, adenocarcinoma; BC, breast carcinoma; Ca., cancer/carcinoma; CRC, colorectal cancer; H&N, head and neck carcinoma; HER2, human epidermal growth factor receptor 2; HR, hormone receptor; HRPC, hormone-resistant prostate cancer; IHC, immunohistochemistry; NSCLC, non-small cell lung cancer; RCC, renal cell renal carcinoma; SCC, squamous carcinoma; SCLC, small cell lung carcinoma; TNBC, triple-negative breast carcinoma.

OBI-992 exhibited antitumor activity in CDX models

The antitumor activity of OBI-992 relative to benchmark ADCs (Dato-DXd and/or SG) was evaluated in CDX models. These studies were conducted at various stages of OBI-992's development. A study in the pancreatic cancer BxPC3 CDX model was the initial study in which we examined the efficacy and dosing regimen of OBI-992, using a weekly dosing schedule to compare OBI-992 with SG and Dato-DXd. The BxPC-3 cell line had the highest TROP2 expression levels (Supplementary Table S2) and the highest sensitivity to OBI-992 relative to other tested cell lines (Supplementary Table S3). Three doses of OBI-992, Dato-DXd, or SG were administered weekly at a dose of 3 mg/kg. OBI-992 and Dato-DXd treatments exhibited a statistically significant antitumor effect (TGI = 101% and 85%, respectively) compared with the vehicle control (Fig. 2A). SG treatment partially suppressed tumor growth (TGI = 54%) that was not statistically significant relative to vehicle control. OBI-992 treatment showed significantly greater antitumor activity than SG treatment.

In the following studies, OBI-992 was administered as a single dose on day 1, as the pharmacokinetic data indicate one dose providing sufficient tumor exposure (24). We analyzed OBI-992 activity in a TROP2 high expression gastric cancer NCI-N87 CDX model. OBI-992 or Dato-DXd was administered as a single dose of 3 or 1 mg/kg. Both OBI-992 and Dato-DXd inhibited tumor growth in a dose-dependent manner (Fig. 2B). At a dose of 3 mg/kg, both OBI-992 and Dato-DXd exhibited a statistically significant antitumor effect (TGI = 110% and 96%, respectively). At a dose of 1 mg/kg, OBI-992 and Dato-DXd partially suppressed tumor growth (TGI = 49% and 53%, respectively; Fig. 2B).

The NSCLC NCI-H1975 and TNBC MDA-MB-231 CDX models were used to examine OBI-992 antitumor activity in cells with moderate TROP2 expression (Supplementary Table S2). OBI-992 or Dato-DXd was administered as a single dose of 3 mg/kg in the NCI-H1975 model and at 10 or 1 mg/kg in the MDA-MB-231 model. For both, SG was administered at 12.5 mg/kg twice weekly for a total of four doses.

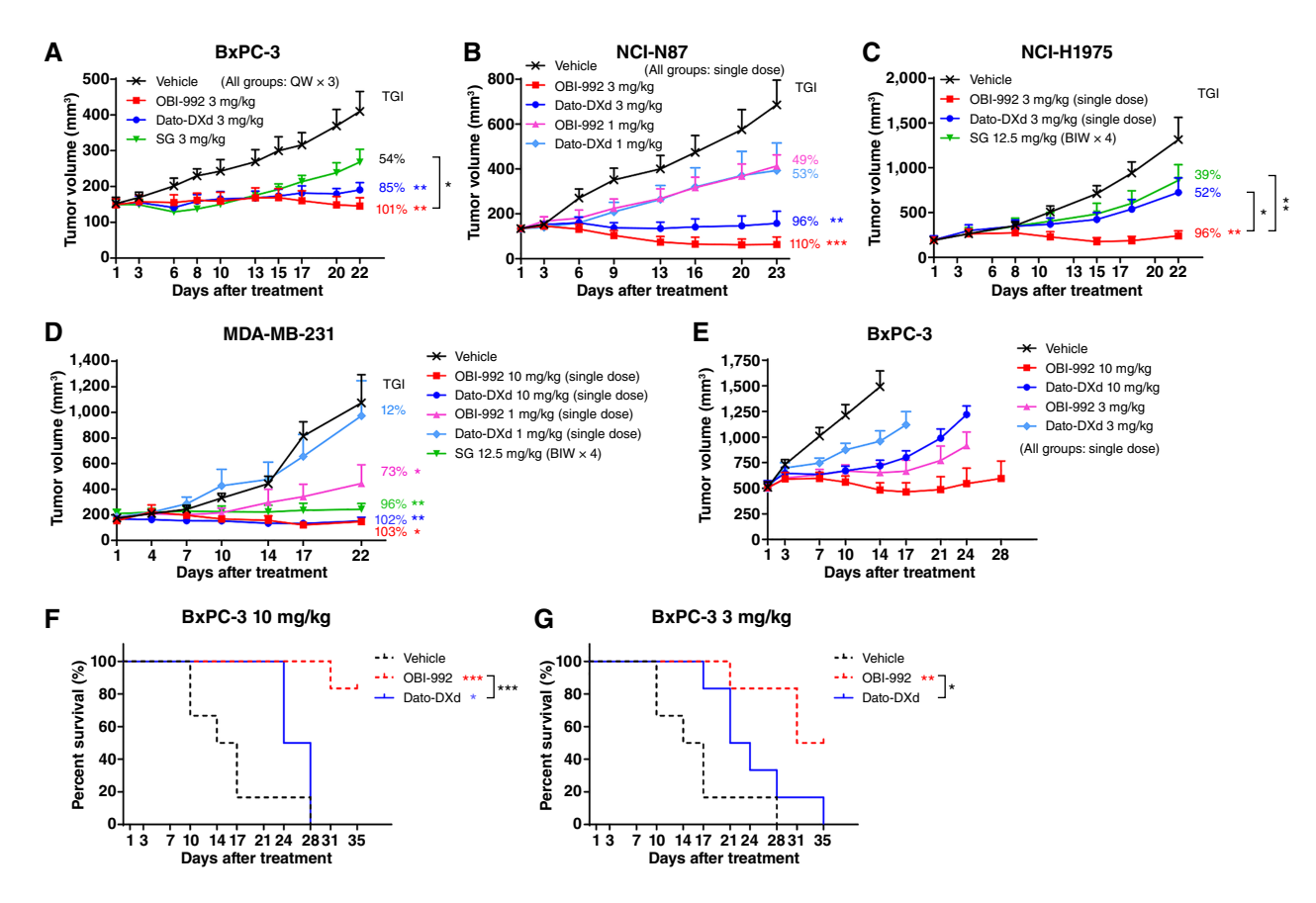


Figure 2. In vivo antitumor activity of OBI-992 on multiple CDX models. Mice were intravenously treated with indicated doses of drugs or vehicle control. A-E, Changes to tumor volume are plotted against number of days after an initial treatment dose for (**A**) BxPC-3 (n = 5 per group), (**B**) NCI-N87 (n = 5 per group), (**C**) NCI-H1975 (n = 6 per group), and (**D**) MDA-MB-231 CDX mice (n = 5 per group) as well as for (**E**) BxPC3 large-tumor CDX mice (n = 6 per group). TGI was calculated for each treatment group and is denoted on the right side of tumor growth plots. F and G, Survival curves were produced for BxPC-3 large-tumor xenograft mice treated with (F) 10 mg/kg or (G) 3 mg/kg OBI-992 or Dato-DXd. *, P < 0.05; **, P < 0.01; ***, P < 0.001 for treatment groups versus vehicle control, unless otherwise noted with a bracket. Dots and error bars indicate the mean ± SEM. All animals survived to scheduled sacrifice with two exceptions: one control animal in C was sacrificed on day 11 due to ulcered tumor, and two OBI-992 (10 mg/kg)-treated mice in D were sacrificed on day 17 due to body weight loss >15%. In large-tumor model (E, F, G), animals were sacrificed if the tumor size exceeded 1,400 mm³ or with ulcered tumor diameter larger than 15 mm. No animals died directly due to tumor burden. BIW \times 4, twice weekly for four doses; Dato-DXd, datopotamab deruxtecan; QW \times 3, once every week for three doses; SG, sacituzumab govitecan; TGI, tumor growth inhibition.

In the NCI-H1975 model, OBI-992 treatment resulted in statistically significant TGI of 96% relative to the vehicle control, whereas Dato-DXd and SG treatments produced partial responses (TGI = 52% and 39%, respectively) that were not significantly different from the vehicle control (Fig. 2C). Furthermore, the TGI of the OBI-992 treatment was significantly greater than those of the Dato-DXd and SG treatments.

In the MDA-MB-231 model, OBI-992 and Dato-DXd showed statistically significant antitumor activity (TGI = 103% and 102%, respectively) relative to the vehicle control at the 10 mg/kg dose (Fig. 2D). However, at the 1 mg/kg dose, OBI-992 showed partial tumor growth suppression (TGI = 73%), which was statistically significant compared with the control, whereas Dato-DXd showed no significant antitumor effect (TGI = 12%; Fig. 2D). In all four CDX models tested, the antitumor activity of OBI-992 was either better than or comparable to that of benchmark treatments.

OBI-992 suppressed tumor growth in a large-tumor model

We further examined the inhibition of tumor growth by OBI-992 in a large-tumor BxPC-3 CDX model. For this model, the tumor volume (450-550 mm³) before treatment initiation was approximately 2.5-fold greater than that in the standard CDX models (150-200 mm³). OBI-992 or Dato-DXd was administered as a single dose of 10 or 3 mg/kg. Both OBI-992 and Dato-DXd treatment suppressed tumor growth, with OBI-992 treatment trending toward having a stronger effect than Dato-DXd (Fig. 2E). Comparing the effects of ADC treatments with the vehicle control was difficult because of the high tumor burden in control mice; three out of six control mice were sacrificed by day 14 posttreatment due to the tumor volume exceeding 1,400 mm³. As a result, the effect of OBI-992 and Dato-DXd on survival of tumor-bearing mice was investigated. Compared with the vehicle control, both OBI-992- and Dato-DXd-treated mice showed significantly better survival at the 10 mg/kg dose (Fig. 2F), but only OBI-992-treated mice had significantly better survival at the 3 mg/kg dose (Fig. 2G). Furthermore, the difference in survival between OBI-992- and Dato-DXdtreated mice at both doses was statistically significant, indicating that OBI-992 had stronger antitumor activity than Dato-DXd in this large-tumor model.

OBI-992 exhibited antitumor activity in PDX models

We further examined the antitumor activity of OBI-992 using PDX models, which retain the heterogeneity and complexity of patient tumors. TROP2 gene expression was confirmed by RNA-seq in several PDX models (Supplementary Table S4). First, we assessed the antitumor activity of OBI-992 in small-scale (n=3 per group) PDX models of breast (BR9464), gastric (GA0091), lung (LU-01-1370), pancreatic (PC-07-0003), esophageal (ES-06-0010), and ovarian (OV-10-0068) cancers. OBI-992 was administered as a single dose of 10 mg/kg. In all six PDX models, OBI-992 treatment inhibited tumor growth, with the greatest effect in the OV-10-0068 model (TGI = 135%), followed by the BR9464, LU-01-1370, PC-07-0003, GA0091, and ES-06-0010 models (TGI = 106%, 105%, 103%, 101%, and 94%, respectively; Fig. 3A–F). The small sample size and diversity of PDX models lead to considerable variation in tumor sizes within control groups, making it difficult to evaluate statistical significance.

Next, we compared the antitumor activity of OBI-992 with Dato-DXd in larger-scale (n=6 per group) PDX models of lung (LU-01-1004 and LU-01-0236) and gastric (GA6866) cancers. OBI-992 or Dato-DXd was administered as a single dose of 10 or 3 mg/kg. In the lung cancer LU-01-1004 model, OBI-992 or Dato-DXd treatment resulted in comparable tumor growth suppression at 10 mg/kg (TGI = 145% and 144%, respectively) and 3 mg/kg (TGI = 91% and

87%, respectively; **Fig. 3G**). In the other lung cancer model (LU-01-0236), OBI-992 treatment resulted in significantly greater growth suppression than Dato-DXd at the 10 mg/kg dose (TGI = 112% and 85%, respectively; **Fig. 3H**). At the 3 mg/kg dose, no significant difference in TGI was observed between OBI-992 and Dato-DXd (TGI = 32% and 30%, respectively; **Fig. 3H**). In the gastric cancer GA6866 model, OBI-992 and Dato-DXd treatment resulted in similar growth suppression at the 10 mg/kg dose (TGI = 110% and 114%, respectively; **Fig. 3I**). At the 3 mg/kg dose, TGI in OBI-992-treated mice (TGI = 111%) was significantly higher than the partial growth inhibition produced by Dato-DXd treatment (TGI = 80%; **Fig. 3I**). Overall, OBI-992 showed comparable or better antitumor activity than Dato-DXd across PDX models.

OBI-992 demonstrated strong bystander killing effects

We evaluated the bystander killing effect of OBI-992 and Dato-DXd using a model of TROP2-positive pancreatic BxPC-3 cells and TROP2-negative ES-2/GFP cells. ES-2/GFP cells alone or cultured with increasing ratios of BxPC-3 cells were treated with OBI-992, Dato-DXd, or a control ADC (human IgG1-exatecan) at increasing concentrations. In control ADC-treated groups, ES-2/GFP cell viability was not notably affected by control ADC treatment or BxPC-3:ES-2/GFP co-culture ratios (Fig. 4C). OBI-992 or Dato-DXd

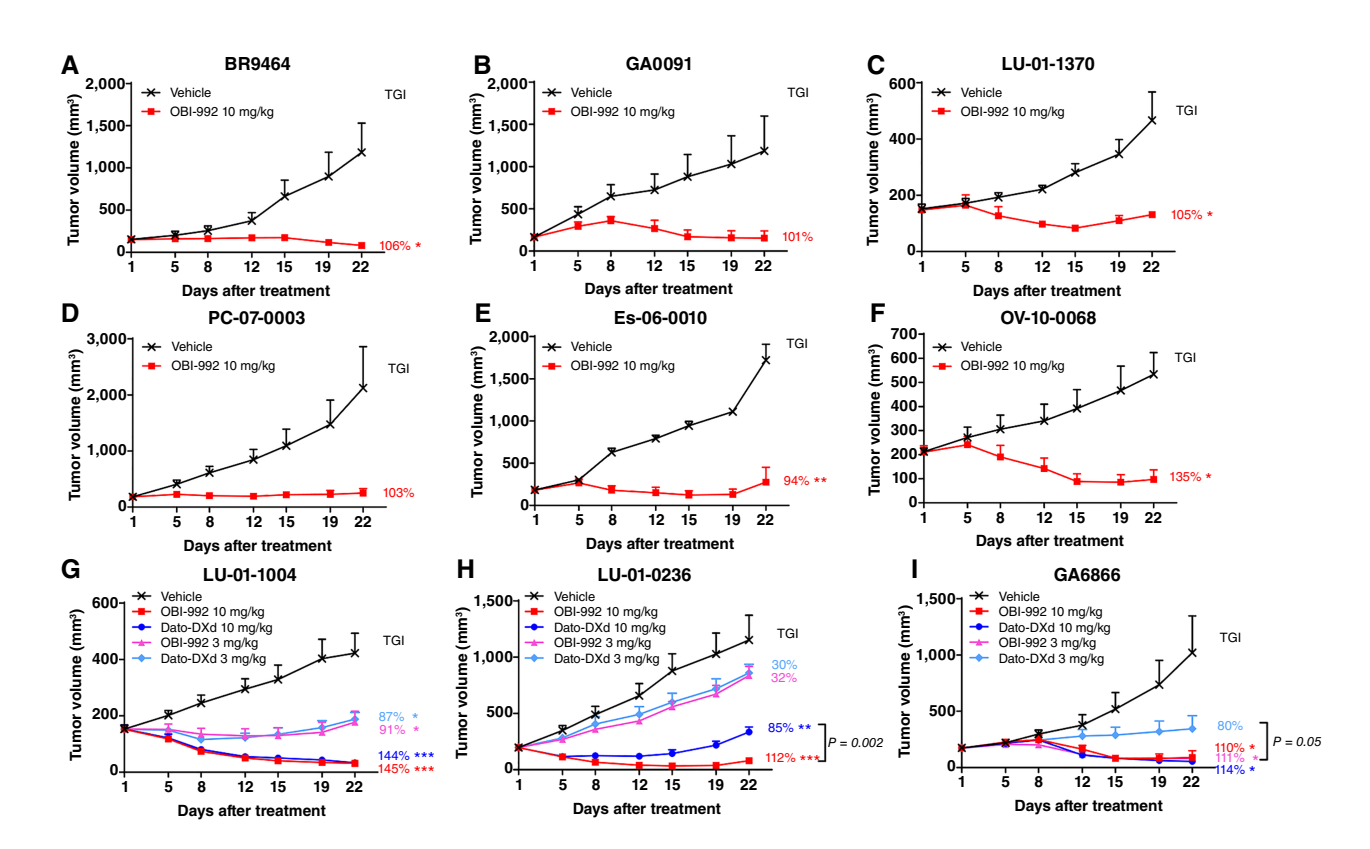
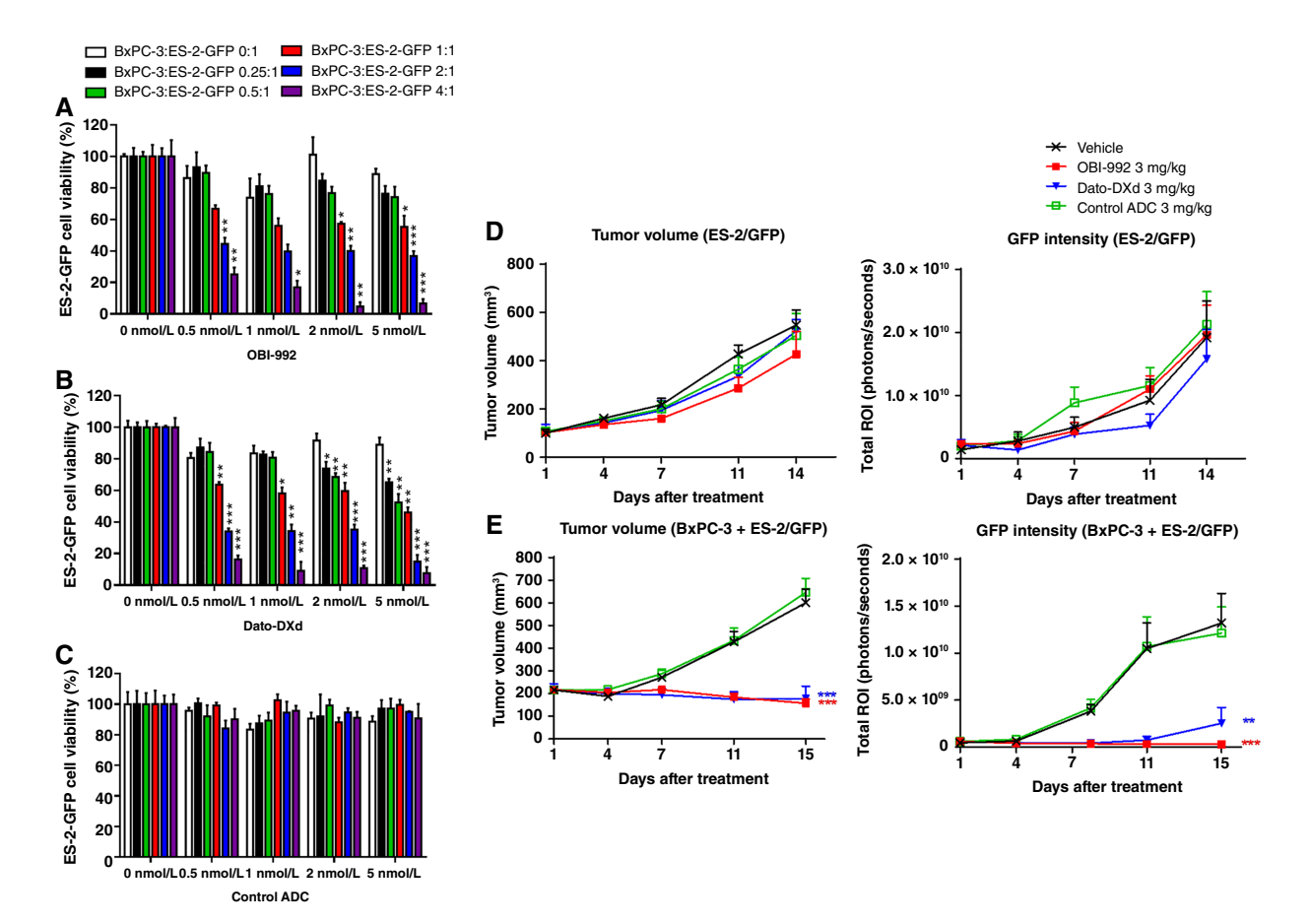


Figure 3. In vivo antitumor activity of OBI-992 on multiple PDX models. Mice were intravenously treated with indicated doses of drugs. Changes to tumor volume are plotted against number of days after an initial treatment dose for (**A**) BR9464 breast cancer, (**B**) GA0091 gastric cancer, (**C**) LU-01-1370 lung cancer, (**D**) PC-07-0003 pancreatic cancer, (**E**) ES-06-0010 esophageal cancer, (**F**) OV-10-0068 ovarian cancer, (**G**) LU-01-1004 and (**H**) LU-01-0236 lung cancer, and (**I**) GA6866 gastric cancer PDX mice. TGI was calculated for each treatment group and is denoted on the right side of tumor growth plots. *, P < 0.05; ***, P < 0.05; ***, P < 0.05; ***, P < 0.05; and (**G-I**) P = 0.0



Bystander killing effect with OBI-992 treatment. A-C, TROP2-positive BxPC3 cells were co-cultured with TROP2-negative ES-2/GFP cells at indicated ratios. The cultures were treated with serially diluted (A) OBI-992, (B) Dato-DXd, or (C) control ADC. Viability of ES-2/GFP cells was measured by the intensity of GFP fluorescence relative to the corresponding non-treated group (0 nmol/L). Dots and error bars indicate the mean \pm SEM (n=3 independent experiments). **D** and E, CDX models of TROP2-negative ES-2/GFP cells (D) alone or (E) mixed with TROP2-positive BxPC-3 cells were treated with vehicle, 3 mg/kg OBI-992, 3 mg/kg Dato-DXd, or control ADC as a single dose. Tumor volume and GFP intensity are plotted against the number of days after treatment. ***, P < 0.001 for treatment groups versus vehicle control. Dots and error bars indicate the mean \pm SEM. ${\bf D}, n=5$ and ${\bf (E)} \ n=10$. All animals survived to the scheduled endpoint. ADC, antibody-drug conjugate; ROI, region of interest; SEM, standard error of the mean.

treatment had little effect on the viability of ES-2/GFP cells in groups with a low ratio of BxPC-3:ES-2/GFP cells (less than 1:1). When the ratio of BxPC-3:ES-2/GFP cells was higher than 1:1, ES-2/ GFP cell viability decreased following OBI-992 or Dato-DXd treatment in a dose-dependent manner (Fig. 4A and B).

The bystander effect was further examined using an in vivo CDX model. A mixture of ES-2/GFP and BxPC-3 cells was used to simulate a tumor with heterogenous TROP2 expression. OBI-992, Dato-DXd, or control ADC was administered as a single 3 mg/kg dose, and tumor volume and GFP intensity (to measure ES-2/GFPspecific tumor growth) were monitored for 2 weeks. In mice with only ES-2/GFP tumors, both tumor volume and GFP intensity were similar in mice treated with vehicle, OBI-992, Dato-DXd, or control ADC (Fig. 4D). In the ES-2/GFP plus BxPC-3 tumor model, tumor volume and GFP intensity were significantly lower with OBI-992 or Dato-DXd treatment than with vehicle and ADC controls (Fig. 4E). Although not reaching statistical significance, OBI-992 exhibited slightly better bystander killing effect than Dato-DXd as measured by GFP intensity. These data indicate that OBI-992 was able to

suppress the growth of tumors composed of a mixture of cells positive and negative for TROP2 expression, suggesting that OBI-992 can exert bystander effects to kill neighboring TROP2-negative

Overexpression of P-gp and BCRP transporters had little impact on OBI-992 activity

Because the multidrug resistance mechanism mediated by ABC transporters plays an important role in ADC resistance (29), we investigated the impact of ABC transporters P-gp and BCRP on TROP2 ADCs and their payloads. We first analyzed the permeability and efflux ratio of several payloads, including exatecan (OBI-992 payload), DXd (Dato-DXd payload), and SN-38 (SG payload). Digoxin and estrone 3-sulfate are known substrates of P-gp and BCRP (30), respectively, and served as controls. The measured efflux ratios indicated that SN-38 and DXd were rapidly pumped out by transporters (efflux ratio >9), whereas exatecan was externalized at a much lower rate (efflux ratio <3; Supplementary Table S5). When measurements were made in the presence of P-gp or BCRP inhibitors (verapamil or Ko143, respectively), all efflux ratios were reduced, indicating that P-gp and BCRP were involved in the observed payload efflux (Supplementary Table S5).

The cytotoxicity of SN-38, DXd, exatecan, and the corresponding ADCs was assessed using HCC827 cell lines with stable over-expression of either P-gp (encoded by *ABCB1*) or BCRP (encoded by *ABCG2*) to mimic multidrug-resistant cancer cells (Supplementary Table S6). Expression levels of *ABCB1* and *ABCG2* were confirmed by qRT-PCR (**Fig. 5A** and **B**). SN-38 cytotoxicity decreased with BCRP overexpression, and DXd cytotoxicity decreased with both P-gp and BCRP overexpression. Conversely, exatecan cytotoxicity was not affected by P-gp overexpression and, compared with SN-38 and DXd, was less affected by BCRP overexpression. The impact of P-gp and BCRP overexpression on the cytotoxicity of ADCs was similar to that observed for the corresponding payload each ADC employs (Supplementary Table S6). Furthermore, the cytotoxicity of SG and Dato-DXd in cells overexpressing BCRP was

restored by the BCRP inhibitor Ko143, whereas in cells over-expressing P-gp, the P-gp inhibitor verapamil restored the cytotoxicity of Dato-DXd but did not notably affect the cytotoxicity of SG, as SN-38 is not a substrate of P-gp (Supplementary Table S7). Both P-gp and BCRP inhibitors had little effect on the cytotoxicity of OBI-992 in HCC827/ABCB1 and HCC827/ABCG2 cells.

The antitumor activity of OBI-992, Dato-DXd, and SG was further evaluated in CDX models of HCC827/ABCB1 and HCC827/ABCG2 stable cell lines, as well as parental HCC827 cells. OBI-992 or Dato-DXd was administered at 10 or 3 mg/kg as a single dose, and SG was administered at 12.5 mg/kg twice weekly for four doses. In the HCC827 model, all tested ADCs exhibited antitumor activity, with TGI higher than 100% at all tested doses (Fig. 5C and D). In the P-gp overexpressing HCC827/ABCB1 model, OBI-992 and Dato-DXd treatment both showed a significant antitumor effect compared with the vehicle control (TGI = 100% and 90%, respectively) when administered at a dose of 10 mg/kg (Fig. 5E). At a dose

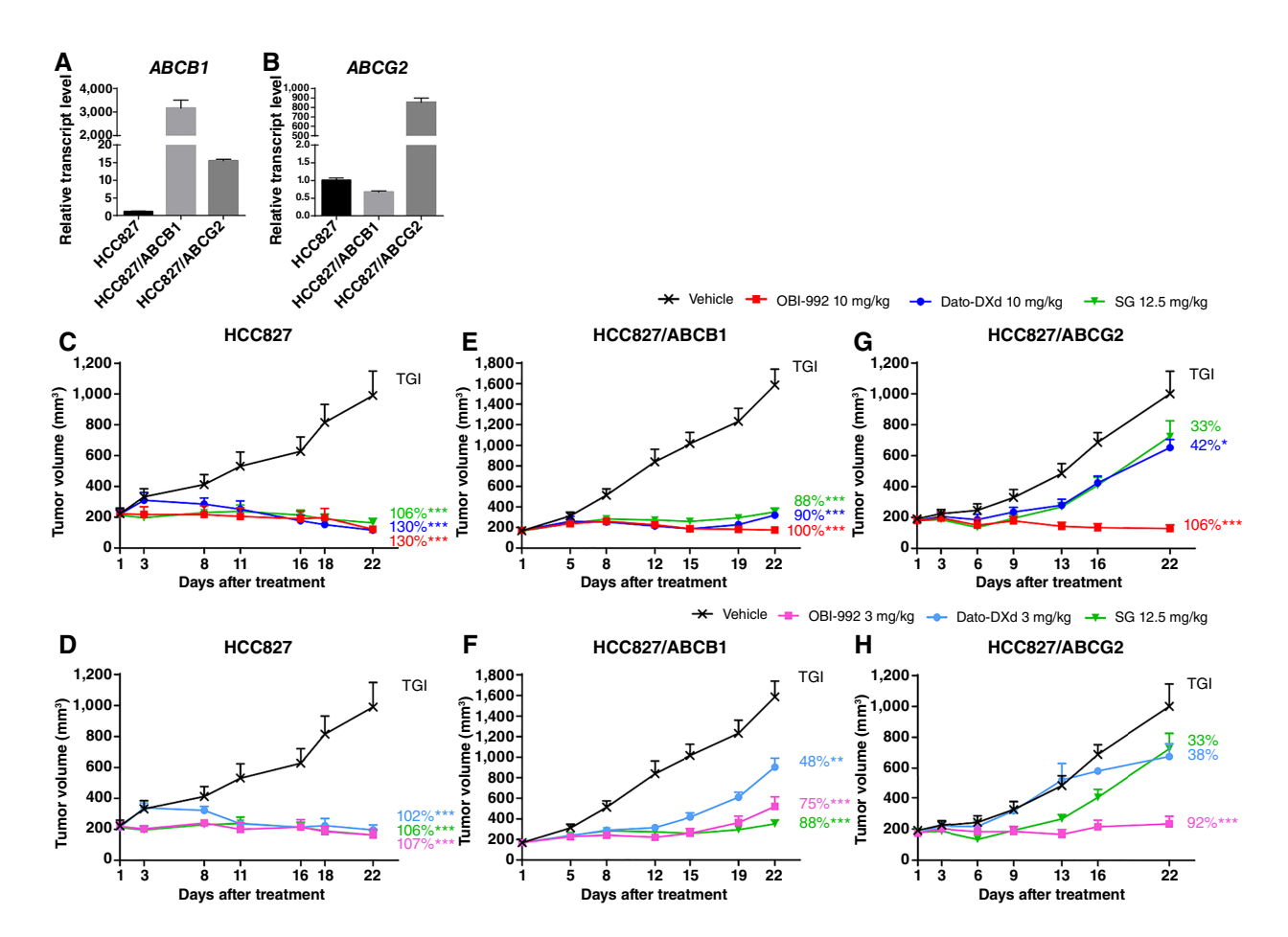


Figure 5.

OBI-992 maintained antitumor activity in both P-gp and BCRP overexpression tumor models. **A,** *ABCB1* (encodes P-gp) and (**B**) *ABCG2* (encodes BCRP) mRNA levels in HCC827, HCC827, HCC827/ABCG2 cells were measured by qRT-PCR. Relative transcript levels are normalized to levels in HCC827 cells. Dots and error bars indicate the mean \pm SEM (n = 3). **C-H,** Mice were intravenously treated with indicated doses of drugs. OBI-992 or Dato-DXd was administered as a single dose on day 1, whereas SG was administered twice a week for four doses. Changes to tumor volume are plotted against number of days after an initial treatment dose for (**C** and **D**) HCC827 (n = 5 per group), (**E** and **F**) HCC827/*ABCB1* (n = 6 per group), and (**G** and **H**) HCC827/*ABCG2* CDX mice (n = 6 per group). TGI was calculated for each treatment group and is denoted on the right side of tumor growth plots. *, P < 0.05; ***, P < 0.01; ***, P < 0.001 for treatment group versus vehicle control. Dots and error bars indicate the mean \pm SEM (n = 5-6). All animals survived to the scheduled endpoint. BCRP, breast cancer resistance protein; Dato-DXd, datopotamab deruxtecan; P-gp, P-glycoprotein; SEM, standard error of the mean; SG, sacituzumab govitecan; TGI, tumor growth inhibition.

of 3 mg/kg, OBI-992 retained a TGI of 75% relative to the vehicle control, whereas Dato-DXd showed partial antitumor activity (TGI = 48%; Fig. 5F). SG treatment had an 88% TGI in this model. In the BCRP-overexpressing HCC827/ABCG2 model, OBI-992 treatment at 10 mg/kg significantly suppressed tumor growth compared with the vehicle control (TGI = 106%), whereas the TGI of Dato-DXd treatment at the same dose was less than half that of OBI-992 (42%; Fig. 5G). At 3 mg/kg, OBI-992 also showed antitumor activity, with 92% TGI versus the vehicle (Fig. 5H). There was no significant inhibition of tumor growth with Dato-DXd at 3 mg/kg. SG treatment also showed a limited TGI of 33% in the HCC827/ABCG2 model (Fig. 5G and H).

OBI-992 in combination with PARP inhibitors produced synergistic antitumor activity

The OBI-992 payload exatecan induces cell death by causing DNA damage. Thus, combining OBI-992 with inhibitors of DNA repair mechanisms, such as PARP inhibitors, may enhance the antitumor activity of the ADC (31, 32). DNA damage can also be repaired by homologous recombination; therefore, cells bearing homologous recombination deficiency (HRD) may be more sensitive to TOP1 and PARP inhibitors (32, 33). Accordingly, we observed a synergistic effect of combined OBI-992 and PARP inhibitor (olaparib and talazoparib) treatment on the viability of HRDpositive Capan-1 cells but not HRD-negative BxPC-3 cell lines. (Fig. 6A and B).

We expanded these findings by evaluating the synergistic effect of OBI-992 and PARP inhibitors in vivo using the HRD-positive pancreatic cancer Capan-1 CDX model. Tumor-bearing mice were administered vehicle, OBI-992 at 0.1 or 0.3 mg/kg, olaparib at 80 mg/kg, talazoparib at 0.1 mg/kg, OBI-992 (0.1 or 0.3 mg/kg) plus 80 mg/kg olaparib, or OBI-992 (0.1 or 0.3 mg/kg) plus 0.1 mg/kg talazoparib. OBI-992 was administered as a single dose, whereas olaparib and talazoparib were administered at 5-day on/2-day off cycles. Suboptimal doses of OBI-992 and PARP inhibitors allowed the synergistic effect of the combination therapy to be easily observed. Partial inhibition of tumor growth was observed in the single treatment groups, with no statistically significant difference compared with the vehicle control (TGI = 31%-41%; **Fig. 6C** and **D**). In contrast, antitumor activity was statistically significant for the combination of OBI-992 at 0.1 or 0.3 mg/kg with either olaparib (TGI = 83% and 98%, respectively; Fig. 6C) or talazoparib (TGI = 97% and 103%, respectively; Fig. 6D) relative to vehicle control. TGI was also significantly greater with either combination therapy (OBI-992 plus olaparib or talazoparib) than with the corresponding treatments of OBI-992 or PARP inhibitors alone, further supporting the benefit of OBI-992 combined with PARP inhibitors.

OBI-992 in combination with an immune checkpoint inhibitor produced enhanced antitumor activity

Immune checkpoint inhibitors have been proposed for combination therapy with ADCs that use TOP1 inhibitors as payloads because TOP1 inhibitors can stimulate the adaptive immune system (31, 34). In mouse colon cancer cells transfected with human TROP2 cDNA (MC38/hTROP2), we found that markers of (ICD) were significantly elevated following treatment with OBI-992 or exatecan relative to untreated controls (Supplementary Fig. S4). To test the hypothesis that combining OBI-992 with immune checkpoint inhibitors would enhance the antitumor activity of the drugs, we created a syngeneic mouse model using MC38/hTROP2 cells. With suboptimal dose(s) of OBI-992 (single 3 mg/kg dose) or an

anti-mouse PD-1 antibody alone (5 mg/kg, twice weekly for a total of three doses), tumor growth was not inhibited (Fig. 6E). In contrast, combined treatment demonstrated significantly greater growth suppression (TGI = 62%) than treatment with vehicle control or OBI-992 alone, suggesting the potential benefits of OBI-992 and PD-1 inhibitor combination therapy.

Discussion

In this study, promising preclinical results supported the clinical development of OBI-992, an ADC composed of a novel TROP2targeted antibody coupled with a TOP1 inhibitor (exatecan) via a hydrophilic, enzymatically cleavable linker. Although some ADC therapies have already shown clinical success, there is a need for further optimization of their clinical utility, which can be modulated by the combination of antibody, linker, and payload (3). Additional avenues of improvement for next-generation ADCs include limiting systemic toxicity and treatment resistance, as well as demonstrating efficacious combination therapy.

OBI-992's potent antitumor activity was demonstrated and compared with benchmark ADCs in both CDX and PDX models, with the PDX results supporting its potential translatability to the clinic (Figs. 2 and 3). Considering the difference in linker/payload design, SG was administered twice a week at a high dose while OBI-992 and Dato-DXd were given as a single injection at lower doses. TGI by OBI-992 was consistently greater than that of SG, the only FDA-approved anti-TROP2 ADC, and was greater than or comparable to the antitumor activity of Dato-DXd. However, given the higher cytotoxicity of exatecan relative to SN-38 and DXd, it may limit OBI-992 dose that can be employed in clinical

Notably, antitumor activity was achieved despite the slower and lower level of internalization of OBI-992 compared with Dato-DXd and SG (T.L. Chang and colleagues; submitted for publication). The slow internalization of ADCs may enhance tissue penetration and increase tumor response, as the rapid internalization has been shown to limit ADC distribution in tumors (35, 36). Several other factors may also contribute to the antitumor activity of ADCs, such as stability during circulation, payload potency, and hydrophilicity of both the linker and the payload. Exatecan as a payload may explain OBI-992's substantial bystander killing effect observed for mixtures of TROP2-postive and TROP2-negative cells in vitro and in vivo (Fig. 4), as exatecan has favorable membrane permeability (37). Other potential benefits of OBI-992 include higher stability in circulation than Dato-DXd, as shown by ex vivo serum stability, which may mitigate off-target toxicities (24). However, the stable linker with a potent payload exatecan could also increase OBI-992's on-target toxicities, which may compromise clinical tolerability and require attentions in clinical study.

ADC payloads, similar to traditional chemotherapy, can be susceptible to the multidrug resistance mechanism that occurs through enhanced drug extrusion by ABC transporter proteins (29). Two ABC transporters, P-gp and BCRP, are commonly overexpressed in treatment-resistant cancers (38, 39). Transporter-mediated treatment resistance to OBI-992 could potentially be mitigated by the payload exatecan, which, as a free drug, has low sensitivity to P-gp/ BCRP overexpression. In the present study, P-gp and BCRP inhibitors and overexpression cell lines were used to assess the potential resistance to OBI-992, SG, and Dato-DXd. In measurements of free payload transport across the plasma membrane, the efflux ratio of exatecan was the lowest overall, independent of P-gp

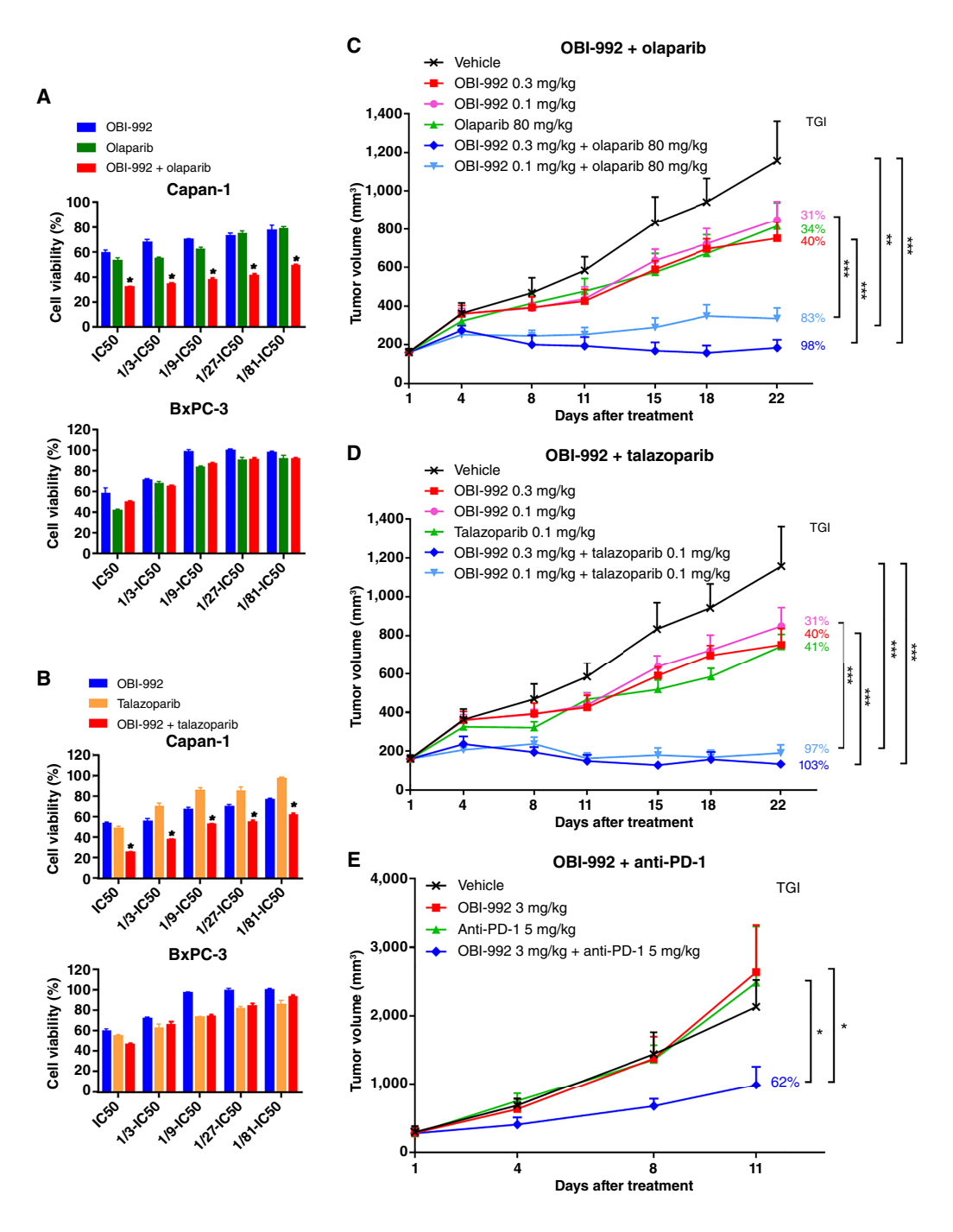


Figure 6. Synergistic antitumor effect of OBI-992 in combination with PARP inhibitors or anti-PD-1 antibody. **A** and **B**, *In vitro* cytotoxicity assay of HRD-positive Capan-1 and HRD-negative BxPC3 cells treated with OBI-992 and/or (**A**) olaparib or (**B**) talazoparib at decreasing doses. The cell viability presented was normalized to a vehicle control. Dots and error bars indicate the mean \pm SEM (n=3 technical replicates). The synergistic biologic activity of OBI-992 in combination with olaparib or talazoparib was examined using CDI as described in "Methods and Materials"; combination groups that showed synergistic effect (CDI <1) were labeled with an asterisk. The calculated CDI values were described in Supplementary Table S8. **C** and **D**, Capan-1 CDX mice were treated with the indicated suboptimal doses of OBI-992 via intravenous injection and/or (**C**) olaparib or (**D**) talazoparib by oral gavage. All animals survived to scheduled endpoint. **E**, Colon cancer MC38/hTROP2 syngeneic mice (immunocompetent B6 mice; n=6 per group) were treated with the indicated suboptimal doses of OBI-992 and/or anti-PD-1 via intravenous injection. The experiment was terminated on day 11 due to rapid tumor growth in the syngeneic model. No tumor rejection was observed in animals. **C-E**, Changes to tumor volume are plotted against the number of days after an initial treatment dose. TGI was calculated for each treatment group and is denoted on the right side of tumor growth plots. *, P < 0.05; ***, P < 0.05; ***, P < 0.001 for the comparisons indicated by brackets. Dots and error bars indicate the mean \pm SEM (n=6). Anti-PD-1, anti-programmed cell death protein 1 antibody; IC₅₀, half-maximal inhibitory concentration; SEM, standard error of the mean; TGI, tumor growth inhibition.

FIRST DISCLOSURE

activity, and least sensitive to BCRP activity (Supplementary Table S5). These results suggest that exatecan is not a substrate of P-gp and a much weaker substrate of BCRP. The cytotoxicity and in vivo xenograft results showed similar trends, as OBI-992 activity was relatively consistent, whereas the activity of SG and Dato-DXd was highly affected by the overexpression of BCRP and/or P-gp (Fig. 5; Supplementary Tables S6 and S7). These results suggest that OBI-992, compared with similar ADCs, may be less sensitive to multidrug resistance.

Several combination therapies have been proposed for TOP1 inhibitor-conjugated ADCs (31). This study evaluated the combinations of OBI-992 with PARP inhibitors and with anti-PD-1 immunotherapy. The rationale for the combination with PARP inhibitors is that cancer cells have several pathways to repair the DNA damage caused by exatecan, including PARP-mediated responses and homologous recombination (32, 33). Cells deficient in homologous recombination (HRD positive) are dependent on PARP-mediated DNA repair and are thus sensitized to PARP inhibition. In this study, the in vitro cytotoxicity of OBI-992 plus PARP inhibitors (olaparib or talazoparib) was dependent on HRD, and this drug combination produced a significant synergistic antitumor activity in an HRD-positive xenograft model (Fig. 6A-D). Therefore, PARP inhibition, particularly in HRD-positive tumors, may promote the exatecan-induced accumulation of DNA damage that leads to cell death. To reduce potential toxicity of OBI-992/ PARP inhibitor combination, dose titration and dose regimen (concurrent vs. sequential dosing) should be further investigated.

The rationale for combining OBI-992 with an immune checkpoint inhibitor is that drug-induced ICD has the potential to activate the immune system to attack tumor cells; however, cells downregulate the immune response by expressing programmed death ligand 1 (PD-L1), the ligand of PD-1 (40). Furthermore, studies have shown that TOP1 inhibition increases PD-L1 expression, suggesting a downregulation of the adaptive immune response by TOP1-targeted treatment alone (34). This downregulation could potentially be blocked via an anti-PD-1 therapy, which promotes antitumor immunity by inhibiting the PD-1/PD-L1 immune checkpoint (40). In this study, both exatecan and OBI-992 treatment led to an increase in ICD markers (Supplementary Fig. S4). Additionally, significant TGI was observed with the combination treatment of OBI-992 and anti-PD-1 antibody in a murine colon cancer model (Fig. 6E). Together, these results suggest that OBI-992 treatment may induce an immune response that is promoted by PD-1 blockade, leading to enhanced tumor-directed immunity with combination therapy.

Anti-TROP2 antibodies have received FDA approval for certain breast cancers (41) and are currently under clinical investigation for NSCLC (42). The IHC results in the present study demonstrated high TROP2 expression in these and additional tumor types, including gynecologic, esophageal, and prostate cancers. Additionally, expression levels were higher in cancerous than in normal tissues in all tissue types except the kidney, which aligns with previous reports (4, 43). Widespread TROP2 expression, together with remarkably consistent OBI-992 antitumor activity across many cancer models, suggests that several of the cancers examined in this study are potential targets for OBI-992 therapy.

In summary, OBI-992 is a clinically relevant ADC that consistently exhibited equal or better antitumor activity than other TROP2-targeted ADCs. A strong bystander effect enabled activity against tumors with heterogeneous TROP2 expression. Moreover, OBI-992 maintained antitumor activity with the overexpression of P-gp or BCRP and showed synergistic activity in combination with PARP and immune checkpoint inhibitors. OBI-992 is under investigation in a phase 1/2 clinical trial (ClinicalTrials.gov: NCT06480240) for individuals with advanced solid tumors.

Authors' Disclosures

W.-F. Li reports a patent for PCT/US2024/021729 pending and a patent 113111546 pending. T.-Y. Huang reports a patent for PCT/US2024/021729 pending and a patent 113111546 pending. M.-T. Lai reports a patent for PCT/US2024/ 021729 pending and a patent for 113111546/Taiwan pending. No disclosures were reported by the other authors.

Authors' Contributions

W.-F. Li: Conceptualization, supervision, writing-original draft, writingreview and editing. M.-F. Chiang: Data curation, visualization, writing-original draft, project administration. H.-C. Weng: Formal analysis, investigation, visualization, methodology. J.-J. Yang: Investigation, methodology. H.-S. Wu: Investigation, methodology. S.-Y. Wu: Investigation. Y.-J. Chen: Investigation, methodology. C.-H. Lu: Investigation, methodology. J.-S. Tu: Investigation, methodology. R.-Y. Hsu: Formal analysis, investigation, methodology. C.-S. Shia: Conceptualization, visualization. T.-Y. Huang: Resources. M.-T. Lai: Conceptualization, writing-review and editing.

Acknowledgments

This work was supported by OBI Pharma, Inc. The authors would like to thank Chun-Chung Wang, Pin-Tzu Chiu, Nan-Hsuan Wang, and Wei-Han Lee for their assistance in this study and Ling-Yi Hung for making the graphical abstract. We thank the National RNAi Core Facility at Academia Sinica in Taiwan for providing the shRNA reagents and related services. Copyediting services were provided by Prescott Medical Communications Group, a Citrus Health Group, Inc. company (Chicago, IL), and funded by OBI Pharma, Inc.

Supplementary data for this article are available at Molecular Cancer Therapeutics Online (http://mct.aacrjournals.org/).

Received July 17, 2024; revised October 14, 2024; accepted December 4, 2024; published first December 30, 2024.

- 1. Fu Z, Li S, Han S, Shi C, Zhang Y. Antibody drug conjugate: the "biological missile" for targeted cancer therapy. Signal Transduct Target Ther 2022;7:93.
- 2. Shastry M, Gupta A, Chandarlapaty S, Young M, Powles T, Hamilton E. Rise of antibody-drug conjugates: the present and future. Am Soc Clin Oncol Educ Book 2023;43:e390094.
- 3. Drago JZ, Modi S, Chandarlapaty S. Unlocking the potential of antibody-drug conjugates for cancer therapy. Nat Rev Clin Oncol 2021;
- 4. Shvartsur A, Bonavida B. Trop2 and its overexpression in cancers: regulation and clinical/therapeutic implications. Genes Cancer 2015;6:84-105.
- 5. Cubas R, Zhang S, Li M, Chen C, Yao Q. Trop2 expression contributes to tumor pathogenesis by activating the ERK MAPK pathway. Mol Cancer 2010;
- 6. Guerra E, Trerotola M, Aloisi AL, Tripaldi R, Vacca G, La Sorda R, et al. The Trop-2 signalling network in cancer growth. Oncogene 2013;32: 1594-600.
- 7. Lenárt S, Lenárt P, Šmarda J, Remšík J, Souček K, Beneš P. Trop2: Jack of all trades, master of none. Cancers (Basel) 2020;12:3328.
- 8. Liao S, Wang B, Zeng R, Bao H, Chen X, Dixit R, et al. Recent advances in trophoblast cell-surface antigen 2 targeted therapy for solid tumors. Drug Dev Res 2021;82:1096-110.

- Chen M-B, Wu H-F, Zhan Y, Fu X-L, Wang A-K, Wang L-S, et al. Prognostic value of TROP2 expression in patients with gallbladder cancer. Tumour Biol 2014;35:11565-9.
- Fong D, Moser P, Krammel C, Gostner JM, Margreiter R, Mitterer M, et al. High expression of TROP2 correlates with poor prognosis in pancreatic cancer. Br J Cancer 2008;99:1290–5.
- Fong D, Spizzo G, Gostner JM, Gastl G, Moser P, Krammel C, et al. TROP2: a novel prognostic marker in squamous cell carcinoma of the oral cavity. Mod Pathol 2008;21:186–91
- Davidson D, Wang Y, Aloyz R, Panasci L. The PARP inhibitor ABT-888 synergizes irinotecan treatment of colon cancer cell lines. Invest New Drugs 2013;31:461-8.
- Mühlmann G, Spizzo G, Gostner J, Zitt M, Maier H, Moser P, et al. TROP2 expression as prognostic marker for gastric carcinoma. J Clin Pathol 2009:62:152–8
- Rowinsky EK. Preclinical and clinical development of exatecan (DX-8951f).
 In: Adams VR, Burke TG, editors. Camptothecins in cancer therapy. Cancer drug discovery and development. 1st ed. Totowa (NJ): Humana Press; 2005.
 p. 317–41.
- De Jager R, Cheverton P, Tamanoi K, Coyle J, Ducharme M, Sakamoto N, et al. DX-8951f: summary of phase I clinical trials. Ann N Y Acad Sci 2000;922: 260-73
- Braybrooke JP, Ranson M, Manegold C, Mattson K, Thatcher N, Cheverton P, et al. Phase II study of exatecan mesylate (DX-8951f) as first line therapy for advanced non-small cell lung cancer. Lung Cancer 2003;41:215–9.
- 17. Royce ME, Rowinsky EK, Hoff PM, Coyle J, DeJager R, Pazdur R, et al. A phase II study of intravenous exatecan mesylate (DX-8951f) administered daily for five days every three weeks to patients with metastatic adenocarcinoma of the colon or rectum. Invest New Drugs 2004;22:53–61.
- Schmitt S, Machui P, Mai I, Herterich S, Wunder S, Cyprys P, et al. Design and evaluation of phosphonamidate-linked exatecan constructs for highly loaded, stable, and efficacious antibody-drug conjugates. Mol Cancer Ther 2024;23: 199–211.
- Bardia A, Mayer IA, Vahdat LT, Tolaney SM, Isakoff SJ, Diamond JR, et al. Sacituzumab govitecan-hziy in refractory metastatic triple-negative breast cancer. N Engl J Med 2019;380:741–51.
- Goldenberg DM, Sharkey RM. Antibody-drug conjugates targeting TROP-2 and incorporating SN-38: a case study of anti-TROP-2 sacituzumab govitecan. MAbs 2019:11:987-95.
- Iyer L, Das S, Janisch L, Wen M, Ramírez J, Karrison T, et al. UGT1A1*28 polymorphism as a determinant of irinotecan disposition and toxicity. Pharmacogenomics J 2002;2:43–7.
- Swain SM, Nishino M, Lancaster LH, Li BT, Nicholson AG, Bartholmai BJ, et al. Multidisciplinary clinical guidance on trastuzumab deruxtecan (T-DXd)related interstitial lung disease/pneumonitis-focus on proactive monitoring, diagnosis, and management. Cancer Treat Rev 2022;106:102378.
- Shimizu T, Sands J, Yoh K, Spira A, Garon EB, Kitazono S, et al. First-in-human, phase I dose-escalation and dose-expansion study of trophoblast cell-surface antigen 2-directed antibody-drug conjugate datopotamab deruxtecan in nonsmall-cell lung cancer: TROPION-PanTumor01. J Clin Oncol 2023;41:4678–87.
- Shia C-S, Wen S-N, Hsu R-Y, Tu J-S, Chang H-W, Li W-F, et al. Abstract 7179: OBI-992, a novel TROP2 targeting antibody drug conjugate demonstrates superior in vivo PK/PD properties and a favorable safety profile. Cancer Res 2024;84(Suppl 6):7179.

- Okajima SNKSD, inventor; Daiichi Sankyo Company Limited, assignee. Method for selectively manufacturing antibody–drug conjugate. Japan patent US 20210386865A1. 2021 Dec 16.
- Soica C, Oprean C, Borcan F, Danciu C, Trandafirescu C, Coricovac D, et al. The synergistic biologic activity of oleanolic and ursolic acids in complex with hydroxypropyl-γ-cyclodextrin. Molecules 2014;19:4924–40.
- Yang M-C, Shia C-S, Li W-F, Wang C-C, Chen I-J, Huang T-Y, et al. Preclinical studies of OBI-999: a novel globo H-targeting antibody-drug conjugate. Mol Cancer Ther 2021;20:1121–32.
- Zhao W, Zhu H, Zhang S, Yong H, Wang W, Zhou Y, et al. Trop2 is overexpressed in gastric cancer and predicts poor prognosis. Oncotarget 2016;7: 6136–45.
- Khoury R, Saleh K, Khalife N, Saleh M, Chahine C, Ibrahim R, et al. Mechanisms of resistance to antibody-drug conjugates. Int J Mol Sci 2023;24:9674.
- Mease K, Sane R, Podila L, Taub ME. Differential selectivity of efflux transporter inhibitors in Caco-2 and MDCK-MDR1 monolayers: a strategy to assess the interaction of a new chemical entity with P-gp, BCRP, and MRP2. J Pharm Sci 2012;101:1888–97.
- Han S, Lim KS, Blackburn BJ, Yun J, Putnam CW, Bull DA, et al. The potential of topoisomerase inhibitor-based antibody-drug conjugates. Pharmaceutics 2022;14:1707.
- 32. Thomas A, Pommier Y. Targeting topoisomerase I in the era of precision medicine. Clin Cancer Res 2019;25:6581–9.
- Stewart MD, Vega DM, Arend RC, Baden JF, Barbash O, Beaubier N, et al. Homologous recombination deficiency: concepts, definitions, and assays. Oncologist 2022;27:167–74.
- Iwata TN, Ishii C, Ishida S, Ogitani Y, Wada T, Agatsuma T. A HER2targeting antibody-drug conjugate, trastuzumab deruxtecan (DS-8201a), enhances antitumor immunity in a mouse model. Mol Cancer Ther 2018;17: 1494–503.
- Nessler I, Khera E, Vance S, Kopp A, Qiu Q, Keating TA, et al. Increased tumor penetration of single-domain antibody-drug conjugates improves in vivo efficacy in prostate cancer models. Cancer Res 2020;80:1268–78.
- Nessler I, Rubahamya B, Kopp A, Hofsess S, Cardillo TM, Sathyanarayan N, et al. Improving intracellular delivery of an antibody-drug conjugate targeting carcinoembryonic antigen increases efficacy at clinically relevant doses in vivo. Mol Cancer Ther 2024;23:343–53.
- Conilh L, Fournet G, Fourmaux E, Murcia A, Matera EL, Joseph B, et al. Exatecan antibody drug conjugates based on a hydrophilic polysarcosine druglinker platform. Pharmaceuticals (Basel) 2021:14:247.
- Amawi H, Sim H-M, Tiwari AK, Ambudkar SV, Shukla S. ABC transportermediated multidrug-resistant cancer. Adv Exp Med Biol 2019;1141:549–80.
- Leonard GD, Fojo T, Bates SE. The role of ABC transporters in clinical practice. Oncologist 2003:8:411–24.
- Ghosh C, Luong G, Sun Y. A snapshot of the PD-1/PD-L1 pathway. J Cancer 2021;12:2735–46.
- 41. Trodelvy. Prescribing information. Foster City (CA): Gilead Sciences; 2020.
- Levy BP, Felip E, Reck M, Yang JC, Cappuzzo F, Yoneshima Y, et al. TRO-PION-Lung08: phase III study of datopotamab deruxtecan plus pembrolizumab as first-line therapy for advanced NSCLC. Future Oncol 2023;19: 1461–72.
- Li Z, Jiang X, Zhang W. TROP2 overexpression promotes proliferation and invasion of lung adenocarcinoma cells. Biochem Biophys Res Commun 2016; 470:197–204.